

## Diffusion of domains on nanometer sized vesicle

Y Sakuma, N Urakami<sup>1</sup>, Y Ogata<sup>1</sup>, M Nagao<sup>2,3</sup>, S Komura<sup>4</sup>, T Kawakatsu<sup>5</sup> and M Imai

Dept. of Physics, Ochanomizu Univ., Tokyo 112-8610, Japan

<sup>1</sup>Dept. of Physics and Information Sciences, Yamaguchi Univ., Yamaguchi 753-8512, Japan

<sup>2</sup>Cyclotron Facility, Indiana Univ., Bloomington, IN 47408-1398, USA

<sup>3</sup>Center for Neutron Research, National Institute of Standards and Technology, Gaithersburg, MD 20899-6102, USA

<sup>4</sup>Dept. of Chemistry, Tokyo Metropolitan Univ., Tokyo 192-0397, Japan

<sup>5</sup>Dept. of Physics, Tohoku Univ., Sendai 980-8578, Japan

sakuma@sweetcream.phys.ocha.ac.jp

**Abstract.** We have investigated the diffusion coefficient of nano-meter-sized domains on a vesicle composed of saturated phospholipids, unsaturated phospholipids and cholesterol by means of neutron spin echo spectroscopy. The obtained diffusion coefficient was examined from a viewpoint of the hydrodynamic model of Brownian objects in a fluid membrane.

### 1. Introduction

In recent years, a lateral phase separation in cell membranes so-called lipid raft has gathered much attention in relation to biological functionalities [1]. Lipid rafts are liquid domains rich in cholesterol, sphingolipid and specific proteins, which might play important roles in the biological processes. Since the biochemical functions may be diffusion controlled [2], the lateral diffusion of lipid rafts in bilayers is of biological interest.

In order to understand the physiochemical nature of lipid rafts, the model giant unilamellar vesicles (GUVs) consisting of saturated lipids, unsaturated lipids and cholesterol have been investigated, because a lateral phase separation of the lipids into a liquid-ordered ( $L_o$ ) phase and a liquid-disordered ( $L_d$ ) phase might be responsible for the formation of rafts in cell membranes. One of the advantages of the model GUV systems is that the domains have the size in micrometer length scale, which makes it possible to observe the phase separation directly by a fluorescence microscopy. Taking this advantage, Cicuta *et al.* [3] estimated the diffusion coefficients of micrometer-sized liquid domains. They found that the liquid-ordered domains diffuse in the liquid-disordered matrix via Brownian motion and the diffusion coefficient,  $D$ , obeys a  $D \propto 1/r$  law in the micrometer length scale, where  $r$  denotes the domain radius.

Based on the hydrodynamic continuum theory, Saffman and Delbrück [4] derived the size dependence of the diffusion coefficient of an object undergoing Brownian motion in the membrane. For the case of  $r < \eta''/\eta_w$  ( $\eta''$ : 2D membrane viscosity and  $\eta_w$ : 3D bulk viscosity of surrounding aqueous phase), the diffusion coefficient is expressed by [4]

$$D(r) = \frac{k_B T}{4\pi\eta''} \left[ \ln\left(\frac{\eta''}{\eta_w} \frac{1}{r}\right) - \gamma + \frac{1}{2} \right], \quad (1)$$

where  $k_B$  is the Boltzmann constant,  $T$  is the temperature and  $\gamma$  is the Euler constant, 0.5772. The 3D membrane viscosity,  $\eta''_{3D}$ , is given by  $\eta''_{3D} \cong \eta''/h$ , where  $h$  is the bilayer thickness. Using typical values for the membranes immersed in water,  $\eta_w \approx 10^{-3}$  Ns/m<sup>2</sup>,  $\eta''_{3D} \approx 10^{-1}$  Ns/m<sup>2</sup> [5] and  $h \approx 5 \times 10^{-9}$  m, we obtain  $\eta''/\eta_w \cong 500$  nm. Thus this logarithmic scaling law is valid for diffusing objects with nanometer-length scale. On the other hand, for the diffusing domains with micrometer-length scale, the diffusion coefficient is expressed by [6]

$$D(r) = \frac{k_B T}{16\eta_w} \frac{1}{r}, \quad (2)$$

which well explains the experimental results reported by Cicuta *et al.*

Since the lipid rafts are believed to have the diameter of 10-100 nm [7], the nanometer-sized domains should obey the  $D \sim \ln(1/r)$  law. In order to confirm the scaling laws, it is desirable to measure the diffusion coefficients of objects in the nanometer scale range. In this study we investigated the dynamics of nanometer-sized domains using a contrast matching technique for neutron spin echo (NSE) and small unilamellar vesicles (SUVs).

## 2. Experiments

### 2.1. Samples

1,2-dioleoyl-sn-glycero-3-phosphocholine (DOPC) (> 99 % purity), 1,2-dipalmitoyl-sn-glycero-3-phosphocholine (*h*-DPPC) (> 99 % purity) and 1,2-dipalmitoyl-d62-sn-glycero-3-phosphocholine (*d*-DPPC) (> 99 % purity) were obtained in a powder form from Avanti Polar Lipid, Inc. Cholesterol (Chol) (> 99 % purity) was purchased from Sigma-Aldrich Co. All lipids were used without further purification and stored 253 K until use [8].

### 2.2. Sample preparations

GUVs were prepared by a gentle hydration method [9]. The obtained GUV suspension was sonicated using an ultrasonic homogenizer with 23kHz frequency (Branson, Sonifire Model 150) for ~20 min. After the sonication the suspension became transparent and we obtained the SUVs.

### 2.3. Measurements

In this study we performed small angle neutron scattering (SANS) experiments under two experimental conditions, one is a film contrast condition where we can obtain whole SUV shape and the other is a contrast matching condition where we can estimate the heterogeneity in the SUVs. The SANS measurements were performed using the SANS-U instrument of ISSP, The University of Tokyo at JRR-3M of the JAEA [10]. In order to obtain the dynamical structure factor of nanometer-sized domains we performed NSE experiments. Since the scattering intensity is low for the matching contrast samples, in this work we concentrated the NSE measurement at  $q = 0.07 \text{ \AA}^{-1}$  and 285 K in order to maximize statistics. The NSE experiments were performed using the NG5-NSE spectrometer at the NIST Center for Neutron Research [11].

## 3. Results and Discussion

First, we characterized the ternary SUVs with the composition of DPPC/DOPC/Chol = 4/4/2 by SANS profiles under the film contrast condition [12]. The obtained SANS profile is well described by the model scattering function for the spherical shell structure. From the fitting we extracted mean outer radius of vesicles  $R_{\text{out}} = (11.2 \pm 0.1)$  nm, the bilayer thickness  $h = (4.2 \pm 0.6)$  nm and the size polydispersity ( $p^2 = \langle R_{\text{in}}^2 \rangle / \langle R_{\text{in}} \rangle^2 - 1$ )  $p = (0.32 \pm 0.02)$ , and these values were independent of the temperature.

The static structure of the nanometer-sized domains on a SUV was examined by the contrast matching technique for SANS. We adjusted the mean scattering length density (SLD) of the homogeneous ternary membrane  $\rho_{d\text{-mix}}$  to that of the solvent  $\rho_{\text{solv}}$ . The obtained SANS profiles for the SUV at the contrast matching condition are shown in figure 1(a). At 333 K in the homogeneous one phase region, we observed no significant scattering from the vesicles, indicating that the lipids are homogeneously mixed in the one phase region and each SUV has the same composition. When we decreased the temperature to the coexisting two-phase region (below 303 K), a scattering maximum due to the phase separation was observed in the vicinity of  $q \cong 0.02 \text{ \AA}^{-1}$  [12, 13, 14]. With decreasing temperature to 285 K, the scattering maximum increases its intensity with keeping the maximum position. We analyzed the observed profiles using a multi-domain model (*e.g.* two domain model is shown in figure 1(b)). The model scattering function of the multi-domain model was calculated by a Monte Carlo simulation technique [12], where we assumed that each domain has the same size and composition. The model scattering function with two domains was well described the observed profile as shown in figure (a), which gave  $\theta_c = 35^\circ$  (corresponding to  $r \sim 8 \text{ nm}$ ).

We examined the dynamics of nanometer-sized domains on the SUV from the intermediate scattering function  $S(q,t)/S(q,0)$  obtained by the NSE measurement. Since the diffusion of domains on a vesicle is composed of two modes, diffusion of the center of gravity of the SUV and that of domains on the SUV, we assumed that the intermediate scattering function of the phase separated SUVs under the matching contrast is expressed by

$$S(q,t)/S(q,0) = A \exp[-D_0 q^2 t] + (1 - A) \exp[-(D_0 + D_d) q^2 t] \quad (3)$$

where  $D_0$  and  $D_d$  are the diffusion coefficients of the whole SUV and the nanometer-sized lipid domain on a SUV, respectively, and  $A$  is a numerical constant. Here we estimated  $D_0$  from the  $S(q,t)/S(q,0)$  of the ternary SUVs at the film contrast condition. The intermediate scattering functions were well described by single exponential functions  $S(q,t)/S(q,0) = \exp(-\Gamma t)$ . The obtained relaxation rates,  $\Gamma$ , at various  $q$  has the relation  $\Gamma = D_0 q^2$  and gives the diffusion coefficient of whole SUV,  $D_0 = (1.31 \pm 0.01) \times 10^{-11} \text{ m}^2/\text{s}$  at 285 K. This value agrees with the diffusion coefficient  $D_{\text{SE}} = 1.14 \times 10^{-11} \text{ m}^2/\text{s}$  calculated by the Stokes-Einstein relation using  $R = 11.2 \text{ nm}$ .

The  $S(q,t)/S(q,0)$  of the ternary SUV at the matching contrast condition is shown in figure 2 with that at the film contrast condition. The difference between  $S(q,t)/S(q,0)$  of the film contrast and that of the matching contrast is attributed to the diffusion of domains in an SUV and the fitting using equation (3) gives the diffusion coefficient of the domains with  $r = 8 \text{ nm}$  as  $D_d = 8.8 \times 10^{-12} \text{ m}^2/\text{s}$ .

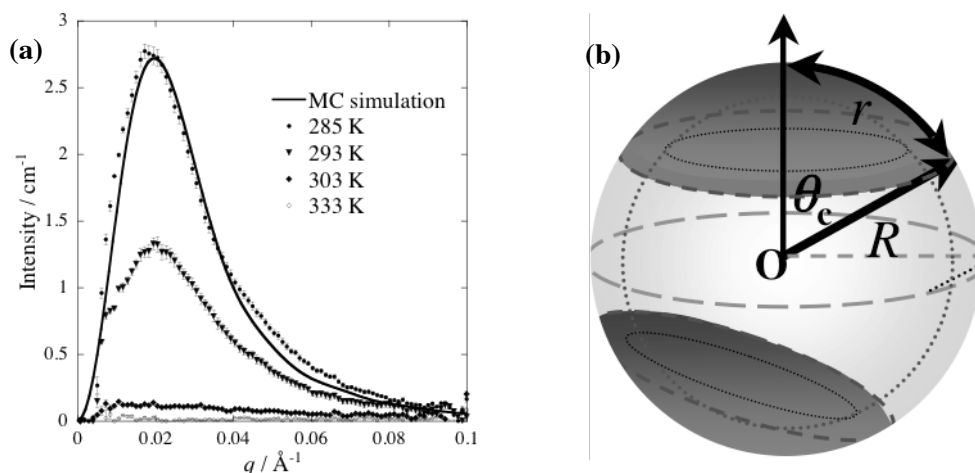


**Figure 1.** (a) Temperature dependence of SANS profiles of binary SUVs at matching contrast condition. Fitting result is shown by solid line. (b) Geometry of two-domain model for Monte Carlo simulations.

In figure 3 we plot the diffusion coefficients of liquid-ordered domains in the liquid-disordered matrix obtained by the NSE measurements (nanometer-scale) and the microscope observation (micrometer-scale) [3] as a function of the radius of the domains. The broken and the solid lines in figure 3 show the  $1/r$  (equation (2)) and the  $\ln(1/r)$  (equation (1)) scaling laws, respectively, where we used  $\eta_w \approx 10^{-3}$  Ns/m<sup>2</sup> and  $\eta_{3D}^* \approx 10^{-1}$  Ns/m<sup>2</sup>. The obtained diffusion coefficient was intermediate between the  $1/r$  and  $\ln(1/r)$  scaling law, indicating the necessity of further experiments to examine the Saffman and Delbrück law quantitatively. On this issue we will address in the forthcoming paper.

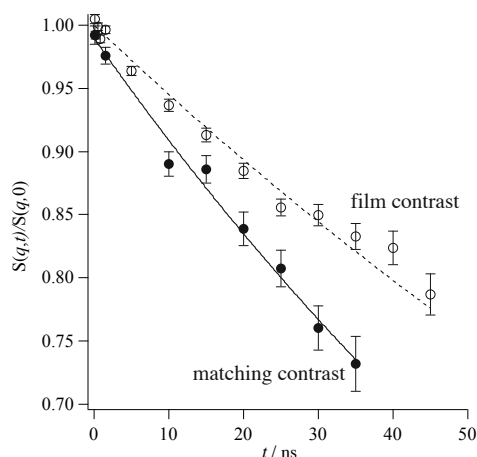


**Figure 2.** Intermediate scattering functions at  $q = 0.07 \text{ \AA}^{-1}$  obtained from NSE experiments. Open circles and closed circles represent the film and the matching contrast experiments, respectively.

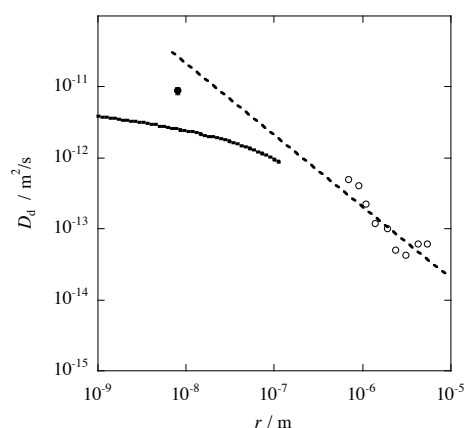


**Figure 3.** Diffusion coefficients of domains as a function of domain radius with  $1/r$  (broken line) and the  $\ln(1/r)$  (solid line) scaling laws. Closed circle and open circles indicate the data from this work and Cicutta *et al.* [3], respectively.

## References

- [1] Simons K and Ikonen E 1997 *Nature* **387** 569
- [2] Hackenbrock C R 1981 *Trends Biochem. Sci.* **6** 151
- [3] Cicutta P, Keller S L and Veatch S L 2007 *J. Phys. Chem. B.* **111** 3328
- [4] Saffman P and Delbrück M 1975 *Proc. Natl. Acad. Sci.* **72** 3111
- [5] Peters R and Cherry R J 1982 *Proc. Natl. Acad. Sci.* **79** 4317
- [6] Hughes B D, Pailthorpe B A and White L R 1981 *J. Fluid Mech.* **110** 349
- [7] Plowman S J, Muncke C, Parton R G and Hancock J F 2005 *Proc. Natl. Acad. Sci.* **102** 15500
- [8] Certain commercial equipment or materials are identified in this paper to foster understanding. Such identification does not imply recommendation by the National Institute of Standards and Technology, nor does it imply that the materials or equipment identified are necessarily the best available for the purpose.
- [9] Reeves J P and Dowben R M 1969 *J. Cell Physiol.* **73** 49
- [10] Ito Y, Imai M and Takahashi S 1995 *Physica B* **213&214** 889
- [11] Monkenbusch M, Schätzler R and Richter D 1997 *Nuclear Instruments and Methods in Physics Research Section A* **399** 301
- [12] Masui T, Urakami N and Imai M, 2008 *Eur. Phys. J. E* **27** 379
- [13] Pencer J, Mills T, Anghel V, Krueger S, Epanand R M and Katsaras J 2005 *Eur. Phys. J. E* **18** 447
- [14] Pencer J, Jackson A, Kucerka N, Nieh M-P and Katsaras J 2008 *Eur. Biophys. J.* **37** 665